ARTICLE NO. 80-4017

Solar Pressure Three-Axis Attitude Control

B. W. Stuck*
Bell Laboratories, Murray Hill, N.J.

The feasibility of two different designs for a three-axis attitude control system is studied for a synchronous-orbit communication satellite. The attitude control is achieved by torques generated by sunlight striking a set of lightweight reflective surfaces called solar sails. The design is studied via analysis as well as a computer simulation of the attitude control dynamics. A nominal trajectory for the satellite attitude is defined, and a set of dynamical equations are derived that are linearized about this nominal trajectory. A sensor scheme is proposed for sensing attitude, and this is combined with the linearized analysis to determine the overall dynamical system behavior for the attitude control system. A sensitivity analysis confirms that the design is robust to unknown disturbance torques and initial conditions far from nominal.

Introduction

IN this paper the feasibility of a particular three-axis attitude control system is studied for a synchronous-orbit communication satellite that uses torques generated from sunlight striking reflecting surfaces called solar sails. The sail orientation can be controlled and this in turn will develop torques to control the satellite spatial orientation. The advantage of such a system over more conventional methods is that fuel for attitude control need not limit the satellite lifetime as it may with alternate designs. Figures 1 and 2 show the two possible designs studied here. Each design has two sets of solar cell panels and a central antenna-electronics body, with three solar sails attached to each solar panel for attitude control. In both designs the antenna rotates about its central shaft every twenty-four hours, minus a factor due to the Earth's annual motion about the sun. In design I the solar panels rotate about their shafts once each year, while in design II the panels wobble from +23.5 deg to −23.5 deg and back again with respect to the antenna shaft once each year. The attitude control problem is to point the antenna Earthward and the solar panels sunward, aligning two prescribed body axes which is equivalent to three-axis attitude control of the solar panels and a prescribed motion of the antenna with respect to the panels. While there are a number of papers in the literature on using solar pressure to control the attitude of a spinning vehicle, which is equivalent to aligning one prescribed body axis, to the best of the author's knowledge that is little or no work available on three-axis attitude control using solar pressure.[1-4]

The technological constraints involved in these designs are dealt with elsewhere.[5-7] From this point on the report will concentrate on the attitude control dynamics of designs I and II and not on systems engineering considerations. In particular, we will deal with effects of disturbance torques on controlling attitude, and will omit problems associated with sail flexing and bending.[8-10] Finally, we assume the sails are sufficiently light that they may be considered massless. Since in fact the sails are not massless, this makes the analysis presented here somewhat optimistic. For the numbers chosen, this is felt to be a reasonable approximation.

Received June 30, 1978; revision received April 18, 1979.

Index category: Spacecraft Dynamics and Control.

*Member of the Technical Staff.

Derivation of Equations of Motions

Assume the solar panels and antenna in each design are ideal rigid bodies with massless interconnecting shafts and solar sails, and the solar panels are identical and rotate in unison about their respective shafts. Fix an inertial right-handed coordinate frame at the center of the sun, with its z-axis normal to the ecliptic and its x-axis pointing at the center of mass of the Earth once a year, at the winter solstice. The dynamical equations of motion for the center of mass decouple from the attitude control equations of motion; since the center-of-mass equations of motion govern orbital stationkeeping, which has received a great deal of attention,[6] it is dropped from this point on.

The attitude control equations of motion for the solar panels are given by

$$\frac{d}{dt}(I_p\omega_p)+\omega_p\times(I_p\omega_p)=N_{\text{sails}}+N_{\text{ant/panel}} \tag{1}$$

where I_p is the solar panel inertia tensor in body-fixed coordinates, ω_p is the panel angular velocity with respect to inertial coordinates, N_{sails} is the sail torque on the solar panels due to the attached sails, and $N_{\text{ant/panel}}$ is the antenna reaction torque on the panels.

In like manner the angular momentum equations of motion for the antenna are

$$\frac{d}{dt}[I_a(\omega_a+\omega_p)]+\omega_p\times[I_a(\omega_a+\omega_p)]=N_{\text{panels/ant}} \tag{2}$$

where I_a is the antenna inertia tensor in body-fixed coordinates, ω_a is the antenna angle velocity in body-fixed coordinates, and $N_{\text{panels/ant}}$ is the total panel reaction torque acting on the antenna.

Adding these equations, and using the fact the reaction torques are equal and opposite, the total angular momentum equation of motion is found to be

$$\frac{d}{dt}[(I_a+2I_p)\omega_p+I_a\omega_a]+\omega_p\times[(I_a+2I_p)\omega_p+I_a\omega_a]=N_{\text{sails}} \tag{3}$$

where N_{sails} is the total sail torque generated on either design by all six sails.

A final kinematical equation is needed to describe how the direction cosines from body-fixed coordinates to inertial coordinates evolve with time:

$$\frac{d}{dt}D_i^{\text{body}}=D_i^{\text{body}}\Omega_i^{\text{body}}$$

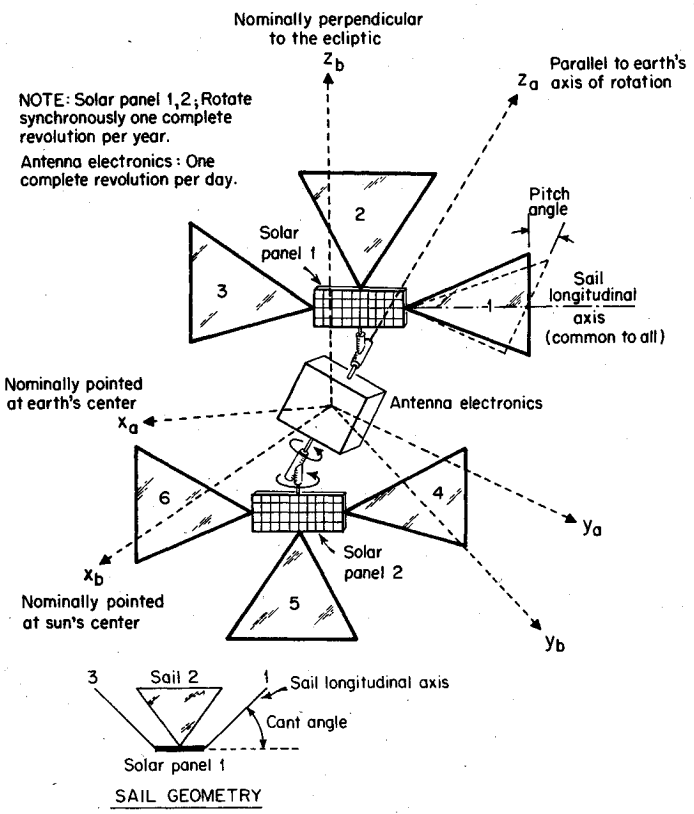

Fig. 1 Design I plus associated coordinate axes.

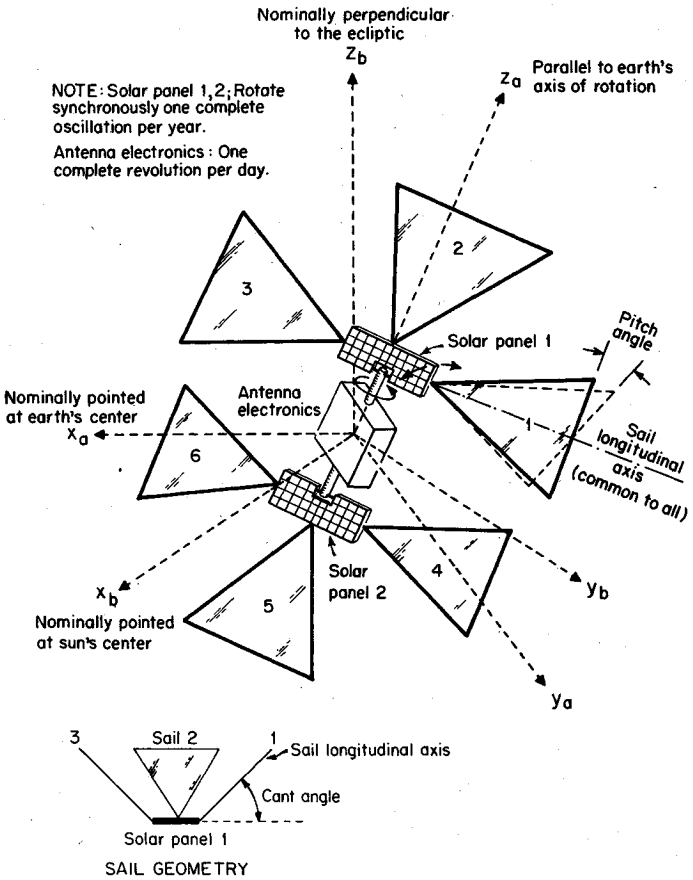

Fig. 2 Design II plus associated coordinate axes.

$$\Omega_i^{\text{body}} = \begin{bmatrix} 0 & -\omega_z & \omega_y \\ \omega_z & 0 & -\omega_x \\ -\omega_y & \omega_x & 0 \end{bmatrix} \tag{4}$$

where D_i^{body} is the 3×3 direction cosine matrix from body-fixed coordinates to inertial coordinates. These equations completely specify the attitude dynamics of designs I and II, given the above assumptions. The inertia tensors of each design as well as a precise explanation of all coordinate frames and coordinate transformations are detailed in Appendices A and B.

Linearization of Equations of Motion

When the direction cosines are perturbed slightly from their nominal values, we see that

$$D_i^{\text{body}} \approx D_{\text{nom}}\,(I+E) \tag{5}$$

where

$$E = \begin{bmatrix} 0 & e_z & -e_y \\ -e_z & 0 & e_x \\ e_y & -e_x & 0 \end{bmatrix} \qquad D_{\text{nom}} = \begin{bmatrix} \cos\psi & -\sin\psi & 0 \\ \sin\psi & \cos\psi & 0 \\ 0 & 0 & 1 \end{bmatrix}$$

where D_{nom} is the nominal direction cosine matrix from body-fixed coordinates to inertial coordinates, I is the 3×3 identity matrix, e_x, e_y, e_z are the infinitesimal rotational errors about actual x, y, and z body-fixed axes, respectively, with respect to each nominal body fixed axis,

$$\psi = (2\pi/365)\,(t-t_0) + \psi_0$$

where t is given in days. Using all this, it is straightforward to show that the actual angular velocity of the body-fixed frame with respect to the inertial frame, and its corresponding angular velocity, can be written as

$$\omega_p \approx \omega_{\text{nom}} + D_{\text{nom}} \frac{de}{dt} \tag{6}$$

$$\frac{d}{dt}\omega_p \approx \frac{d}{dt}\omega_{\text{nom}} + \omega_{\text{nom}} \times D_{\text{nom}} \frac{d}{dt} e + D_{\text{nom}} \frac{d^2}{dt^2} e \tag{7}$$

where $e(e_x, e_y, e_z)$, $\omega_{\text{nom}} = (0,0,-2\pi/365)$, $\omega_{\text{nom}} = (0,0,0)$.

The sail torque can be expanded in a series, including only the nominal torque and a first-order perturbation:

$$N_{\text{sails}} \approx N_{\text{nom}} + D_{\text{nom}} N_{\text{body}} \tag{8}$$

where N_{nom} is the nominal sail torque, hopefully zero as will be shown, and N_{body} is the sail torque beyond nominal torque, in body-fixed axes. Substituting all this into the total equations of motion, and including only terms to first order in linearized variables, and equating nominal trajectory variables to one another and perturbational variables to each other, the linearized equations of motion are found to be

$$\begin{aligned} I_{\text{sat}} \Big[& \omega_{\text{nom}} \times D_{\text{nom}} \frac{de}{dt} + D_{\text{nom}} \frac{d^2 e}{dt^2} \\ & + 2(\Omega_{\text{nom}} I_{pm} - I_{pm} \Omega_{\text{nom}}) D_{\text{nom}} \frac{de}{dt} \\ & + (\Omega_b^q I_{ab} - I_{ab} \Omega_b^q) D_{\text{nom}} \frac{de}{dt} + \omega_{\text{nom}} \times I_{\text{sat}} D_{\text{dom}} \frac{de}{dt} \\ & + D_{\text{nom}} \frac{de}{dt} \times (2 I_{pm} \omega_{\text{nom}} + I_{ab} (\Omega_b^q + \Omega_{\text{nom}}) \Big] \approx D_{\text{nom}} N_{\text{body}} \end{aligned} \tag{9}$$

where

$$I_{\text{sat}} = I_{ab} + 2I_p$$

and

$$\Omega_b^q = \begin{bmatrix} 0 & \omega_{az} & -\omega_{ay} \\ -\omega_{az} & 0 & \omega_{ax} \\ \omega_{ay} & -\omega_{ax} & 0 \end{bmatrix} \tag{10}$$

where ω_{ax}, ω_{ay}, ω_{az} are the components of the antenna angular velocity, and I_{pm} and I_{ab} are inertia tensors defined in Appendix B.

Two simplifying assumptions can now be made. The first is that the gyroscopic coupling of the satellite angular momentum with the angular momentum due to the annual rotation of the solar sails about their shafts is negligible, or

$$I_{\text{sat}} D_{\text{nom}} \frac{d^2 e}{dt^2} \gg I_{\text{sat}} \left(\omega_{\text{nom}} \times D_{\text{nom}} \frac{de}{dt} \right) + 2(\Omega_{\text{nom}} I_{pm} - I_{pm} \Omega_{\text{nom}}) D_{\text{nom}} \frac{de}{dt} - 2I_p \omega_{\text{nom}} \times D_{\text{nom}} \frac{de}{dt} + \omega_{\text{nom}} \times I_{\text{sat}} D_{\text{nom}} \frac{de}{dt} \tag{11}$$

The second is that the gyroscopic coupling of the satellite angular momentum vector with the angular momentum due to the daily rotation of the antenna about its shaft is neglected, or

$$I_{\text{sat}} D_{\text{nom}} \frac{d^2 e}{dt^2} \gg (\Omega_b^q I_{ab} - I_{ab} \Omega_b^q) D_{\text{nom}} \frac{de}{dt} + D_{\text{nom}} \frac{de}{dt} \times I_{ab} (\omega_b^q + \omega_{\text{nom}}) \tag{12}$$

Both approximations can be summarized by the statement that the sail torques are assumed to be capable of correcting the gyroscopic disturbance torques caused by antenna rotation about its shaft once a day and the solar panel rotation about their shafts. These assumptions will be checked later and shown to be self-consistent. Thus, the approximate equations of motion for the linearized variables are

$$I_{\text{sat}} D_{\text{nom}} \frac{d^2 e}{dt^2} \approx D_{\text{nom}} N_{\text{body}} \tag{13}$$

This is the fundamental result of this section. Note that if an x torque is generated in body-fixed axes, the off-diagonal entries in the matrix premultiplying N_{body} will couple this torque into the y axis. Cross-coupling torques between the x and y axes are unavoidable, because of the coordinate transformations between inertial and body-fixed axes, and on physical grounds. To minimize their effects, one straightforward simple method is to demand that the diagonal entries in I_{sat} must be chosen comparable to one another.

Sensor Measurements

Provided all pointing errors are small, Earth sensors and sun sensors detect the center of the Earth and sun, respectively, in body-fixed coordinates. Since e is defined as the pointing error of actual body-fixed axes with respect to nominally sun-pointing coordinates, the components of e have the following physical significance: e_x is the rotation about the body-fixed x axis, i.e., rotation about the sun line; e_y is rotation about the body-fixed y axis, i.e., moving up and down with respect to the center of the sun; e_z is the rotation about the body-fixed z axis, i.e., moving right-left with respect to the center of the sun. Sun sensors measure e_y and e_z directly, but provide no information about e_x.

Earth sensors must be used to find e_x indirectly. Consider the direction cosines from the nominally Earth-pointing coordinate frame to antenna principal axes frame, D_a^e:

$$D_a^e \approx \begin{bmatrix} 1 & -\tilde{e}_z & \tilde{e}_y \\ \tilde{e}_z & 1 & -\tilde{e}_x \\ -\tilde{e}_y & \tilde{e}_x & 1 \end{bmatrix} \tag{14}$$

where $\tilde{e}_x, \tilde{e}_y, \tilde{e}_z$ are the rotation errors of actual antenna principal axes with respect to nominal Earth-pointing axes. Using standard Euler angle coordinate frame rotations to go from antenna principal axes to body-fixed axes (see Appendix A), it is straightforward to show that

$$e_x = \tilde{e}_z (\sin\psi \cos\phi + \cos\psi \cos\theta \sin\phi) - \tilde{e}_y \sin\theta \sin\phi \tag{15a}$$

$$e_y = \tilde{e}_z (\sin\psi \sin\phi + \cos\psi \cos\theta \cos\phi) - \tilde{e}_y \sin\theta \cos\phi \tag{15b}$$

$$e_z = \tilde{e}_z \cos\psi \sin\theta - \tilde{e}_y \cos\theta \tag{15c}$$

Since $\tilde{e}_y$ and $\tilde{e}_z$ are observable using Earth sensors, they can be used to calculate e_x; as a bonus, Earth sensor measurements provide a check on e_y and e_z measurements, and vice versa. These statements are valid provided the trigonometric weighting terms are not zero.

Two effects complicate sensor measurements. First, both sensor noise and amplifier noise corrupt measurements, and second, since solar pressure dynamics are extremely slow, it is probably not necessary to continuously monitor satellite attitude, but rather to sample it at a rate much faster than any disturbances. We choose to ignore these effects here, and will include them in the simulation of the actual equations of motion to show that they can be negligible.

If we assume that gyroscopes were available for monitoring attitude, a different set of assumptions concerning what quantities are observable would be made, and again we choose to ignore this here.

Solar Sail Torques

Appendix C derives the exact torque generated by each sail, under the assumption of no sail shadowing, no radiation falling on the rear of the sails, and small attitude pointing errors.

The force acting on a triangular sail such as in designs I and II can be represented as a vector acting at a point two-thirds of the distance out the longitudinal sail axis, and this point is called the sail center of pressure, while the distance from the sail hinge to the center of pressure will be called the center of pressure lever arm or sail lever arm.

Solar pressure has three distinct components[11]: 1) reflected solar pressure, the largest of the three, directed normal to the surface which sunlight strikes; 2) absorbed solar pressure, next largest of the three, directed along the sun line; and 3) reradiated or thermal solar pressure, smallest of the three, directed normal to the surface which sunlight strikes.

Three simplifying assumptions are now made. First, reflected solar pressure is the only contributor to sail torque. Second, if we denote the pitch angle for sail k by b_k, then $|b_k| \ll 1$. Third, the inner product of the sail k normal with the sun vector in body-fixed coordinates is approximately the same for all sails, or in other words, the projection of each sail's normal along the sun line is roughly the same. Combining all these assumptions together, it can be shown that

$$N_{\text{body}} \approx A(1-E_s)(2I/c)(n \cdot s)^2 [b_1 - b_3 + b_4 - b_6] l_s \cos(a) u_x + (b_1 + b_3 + b_4 + b_6) l_s \sin(a) u_y$$

$$-(b_2+b_5)l_s\sin(a)u_z+(b_1+b_3-b_4-b_6)ru_z$$

$$+(b_3+b_6-b_1-b_4)ru_\psi+(b_2+b_5)u_s \qquad (16)$$

$$u_\psi=\begin{bmatrix}\sin\psi\\ \cos\psi\\ 0\end{bmatrix} \quad u_s=\begin{bmatrix}z+h-l_s\cos(a)+2r\sin(a)\\ 0\\ -r\cos a\end{bmatrix}$$

where A is the area of a sail, with all sails assumed identical, E_s is the emissivity of the sail surface, I is the sunlight pressure constant which is assumed to be 1380 W/m^2, c is the speed of light in vacuum, a is the sail cant angle which is assumed to be 45 deg, l_s is the distance ffrom the sail hinge on the solar panel to the center of pressure of the sail, r is the radius of gyration of the solar panel, h is the distance from the antenna center of mass to the solar panel center of mass, y is the half-length of a solar panel, and z is the half-width of solar panel (see Appendix C), while u_x, u_y, u_z are x,y,z unit vectors respectively. All vectors are measured in body-fixed coordinates.

Three cases of interest now arise.

Case I: X Torque Generation

For the first case, we set $b_1=-b_3=b_4=-b_6-b_0$, $b_2=b_5=0$ and find that the resulting torque is

$$N^I_{\text{body}}\approx A(1-E_s)(2I/c)(n\cdot s)^2[4b_0l_s\cos(a)u_x] \qquad (17)$$

Case II: Y Torque Generation

For the second case, we set $b_1=b_3=b_4=b_6=b_0$, $b_2=b_5=0$ and find that the resulting torque is

$$N^{II}_{\text{body}}\approx A(1-E_s)(2I/c)(n\cdot s)^2 4b_0l_s\sin(a)u_y] \qquad (18)$$

Case III: Z Torque Generation

For the third case, we set $b_1=b_3=b_4=b_6=0$, $b_2=b_5=-b_0$ and find the resulting torque to be approximated by

$$N^{III}_{\text{body}}\approx A(1-E_s)(2I/c)(n\cdot s)^2[2b_0(r\cos(a)$$

$$+l_s\sin(a))u_z-2b_0(z+h-l_s\cos(a)+r\sin(a))u_x] \qquad (19)$$

For all three cases, if the sails are designed such that

$$l_s\cos(a)\gg r\sin(a) \qquad l_s(a)\gg r\sin(a) \qquad (20)$$

then x,y,z torques can be generated in body-fixed axes, by cases I, II, III respectively, as is clear from the above equations or on physical grounds. Sails 1, 3, 4, and 6 produce either x or y torques at any time instant, but not simultaneously, while sails 2 and 5 produce z torques.

Solar Sail Control Law

At this point the analysis of the linearized equations of motion has been reduced to a previously solved problem. Two standard control laws will now be discussed.[12,13] Cross-coupling torques will be assumed negligible throughout this section.

If it were possible to generate simultaneously three independent torques, the attitude error and its first derivative could be used in a control law, e.g.,

$$N_{\text{body}}=N^I_{\text{body}}\text{sign}\left(e_x+k_x\frac{de_x}{dt}\right)$$

$$+N^{II}_{\text{body}}\text{sign}\left(e_y+k_y\frac{de_y}{dt}\right)+N^{III}_{\text{body}}\text{sign}\left(e_z+k_z\frac{de_z}{dt}\right) \qquad (21)$$

where k_x,k_y,k_z are constants chosen to optimize performance within this class of control laws. However, since x and y torques cannot be simultaneously generated, one possible modification to the above control law is

$$\text{if} \quad \left|e_x+k_x\frac{de_x}{dt}\right|\geq\left|e_y+k_y\frac{de_y}{dt}\right| \quad \text{generate } x \text{ torque} \qquad (22)$$

$$\text{if} \quad \left|e_x+k_x\frac{de_x}{dt}\right|<\left|e_y+k_y\frac{de_y}{dt}\right| \quad \text{generate } y \text{ torque} \qquad (23)$$

Finally, if a deadband is included in the control law for each axis, every *sign* function is replaced by a *deadband* function where db denotes the deadband range and

$$\text{deadband}(x)=\begin{cases}\text{sign}(x) & |x|\geq db\\ 0 & |x|<db\end{cases} \qquad (24)$$

These equations with deadbands completely specify a possible control law for either design I or II. The gains k_x, k_y, k_z allow the designer to trade ringing and overshoot in the system transient response for the period of a limit cycle when the satellite is in its nominal trajectory.

Disturbance Torques

Five sources of disturbance torques, in addition to the cross-axis coupling torques already mentioned, can drive design I or II away from nominal attitude. The largest disturbance is due to the Earth's gravitational field trying to align the satellite's longest axis along a line pointing to the Earth's center of mass.[14] The next largest disturbance is caused by sunlight reflecting, absorbing, and reradiating from the satellite (the antenna in particular).[11] The third largest is caused by the satellite center of mass being misaligned. Fourth is micrometeoroid impact torques.[15] Finally, the smallest disturbance torques are due to the satellite interacting with the Earth's magnetic field; these magnetic torques are ignored here.

Gravitational torques on an arbitrary rigid body are straightforward to calculate.[14] It can be shown that

$$N^E_{\text{gravity gradient}}\approx 3\omega_0^2\begin{bmatrix}0\\ -I_{xz}\\ I_{xy}\end{bmatrix} \qquad (25)$$

where $\omega_0=2\pi/24$ rad/h is the satellite orbital frequency, I_{xy}, I_{xz} are off-diagonal elements in the satellite inertia tensor computed in Earth-pointing coordinates, and $N^E_{\text{gravity gradient}}$ are the satellite gravity gradient torques in Earth-pointing coordinates. If we define I^E_{sat} as the satellite inertia tensor in Earth-pointing coordinates, and A^{body}_E as the direction cosines from body-fixed axes to Earth-pointing axes in body-fixed axes, then

$$I^E_{\text{sat}}=A^{\text{body}}_E I_{\text{sat}}A^E_{\text{body}} \qquad (26)$$

The gravity gradient torques in body-fixed axes can be written as

$$N^{\text{body}}_{\text{gravity gradient}}\approx A^E_{\text{body}}N^E_{\text{gravity gradient}} \qquad (27)$$

and are plotted for design I, in body-fixed axes, in Fig. 3a, under the assumption the satellite is moving in its nominal trajectory.

Sunlight pressure torques due to the antenna electronics body are calculated explicitly in an appendix. The reflected and absorbed sunlight pressure torques are plotted in body-fixed axes in Figs. 3b and 3c under the assumption the satellite is moving on its nominal trajectory. More information must be known before the reradiated torque can be calculated explicitly; the best available information suggests this is negligible compared to the other torques discussed here.

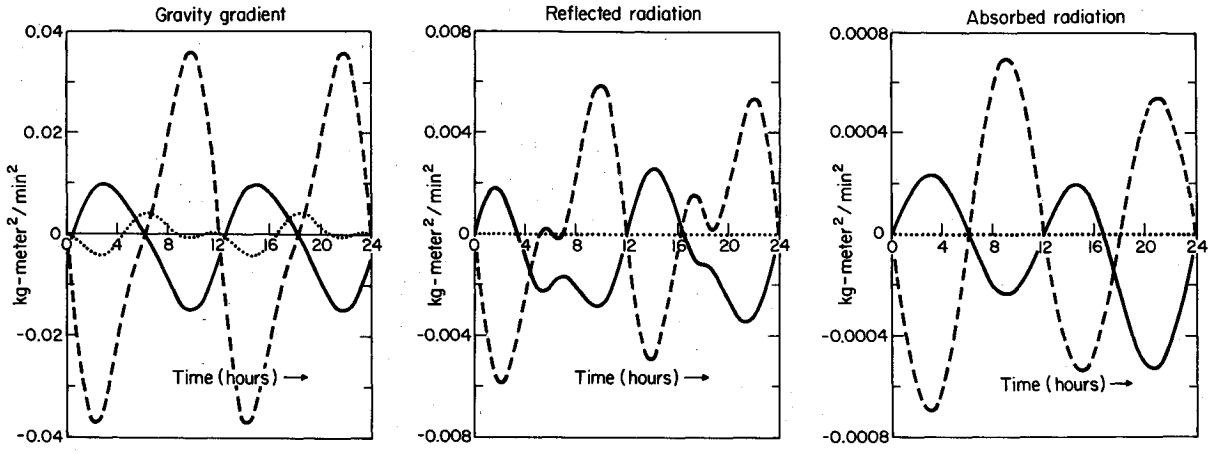

a) Gravity gradient b) Reflected radiation c) Absorbed radiation

Fig. 3 Disturbance torques for design I: (· · ·), x torque; (——)y torque; (– – –)z torque.

Table 1 Control law parameters

Deadband (x,y,z axes)	0.1 deg
$K_x = K_y$ gain	30 min/rad
K_z	40 min/rad
Sensor noise mean (x,y,z axes)	0 deg
Sensor noise standard deviation (x,y,z axes)	0.03 deg

Table 2 Design I weight summary, lb

Antenna	25
Poer control	23
Batteries	50
Electronics	80
Attitude control	25
Structure	25
Contingency	19
Antenna electronics total	247
Bearing drive	15
Solar cells	45
Electronics	10
Cables	8
Structure	25
Contingency	19
Solar cells panel total	122

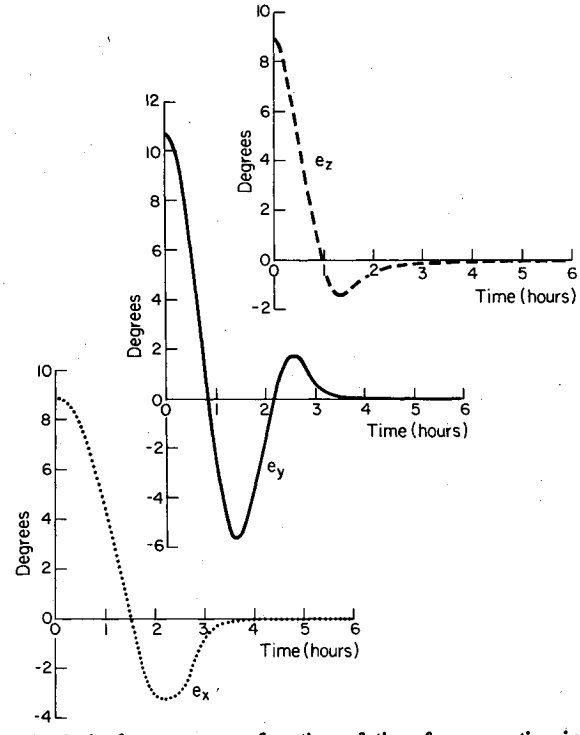

Fig. 4 Attitude errors as a function of time for correcting initial attitude error for design I.

The calculation of center of mass misalignment torques, torques due to the center of mass of the satellite not coinciding with the center of mass of the antenna, is straightforward:

$$N_{cm} = R_{a-cm} \times F_{\text{sails}} + M_{\text{sat}} [2R_{a-cm} \times (\omega_p \times R_{cm}) + R_{a-cm} \times (\omega_a \times R_{cm})] \quad (28)$$

where N_{cm} are center of mass misalignment torques in body-fixed axes, R_{a-cm} is the vector from the antenna center of mass to the actual satellite center of mass, ω_p is the satellite angular acceleration in body-fixed axes, and ω_a is the antenna angular acceleration in body-fixed axes. A typical magnitude for R_{a-cm} is 0.25 in. Since sail torque is proportional to the sail center of pressure lever arm, the sails must be designed such that the sail torque is much greater than the center of mass misalignment torque, that is

$$l_s A (1 - E_s)(2I/c) \gg M_{\text{sat}} |R_{a-cm}|^2 [2|\omega_p| + |\omega_a|] \quad (29)$$

$$l_s \cos(a) \gg |R_{a-cm}| \qquad l_s \sin(a) \gg |R_{a-cm}| \quad (30)$$

A study has been carried out to verify that if the sail cant and pitch angles are offset slightly from their nominal values, the resulting disturbance torques are negligible compared to the attitude correcting torques. This is discussed in the next section.

Finally, the largest expected micrometeoroid appear to be two orders of magnitude less than the attitude correcting torques and hence are assumed negligible.[15]

Computer Simulation Results

As a check on the foregoing analysis, a compter program was written to simulate the dynamics and kinematics of either design I or II. Figures 4-6 show the results of a simulation of design I recovering from an initial pointing error. The initial error was due to the satellite being rotated away from its nominal attitude by three successive rotations of 10 deg each, first about the z axis, then the y axis, and finally the x axis. Sun and Earth sensor measurements are corrupted by additive

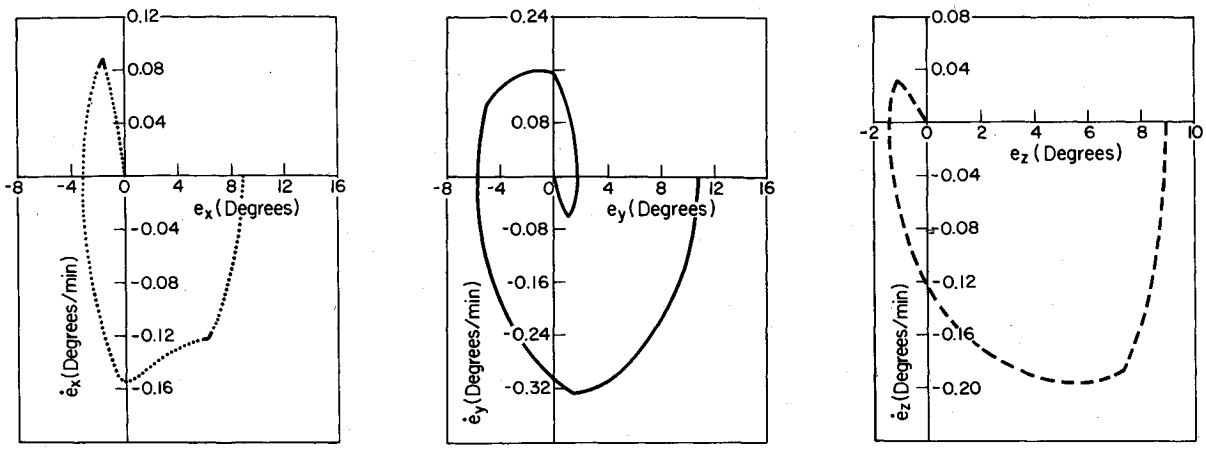

Fig. 5 Pointing error and its rate of change for same initial error as in Fig. 4 for design I.

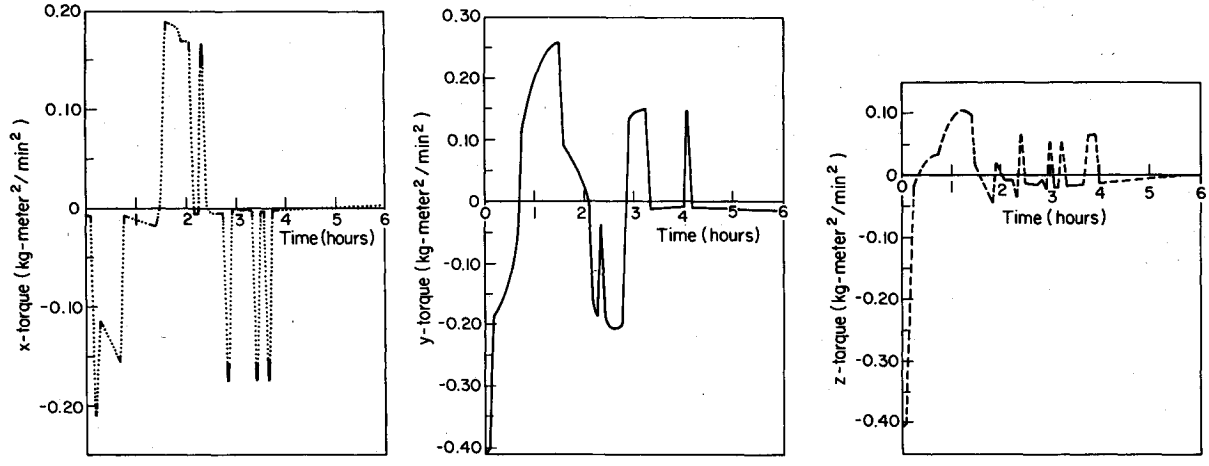

Fig. 6 Torques as a function of time for same initial error as in Fig. 4 for design I.

Table 3 Design I inertia tensor components, kg – m^2

Antenna		Solar cells	
I_{axx}	300	I_{xx}	964
I_{ayy}	225	I_{yy}	482
I_{azz}	225	I_{zz}	482

Table 4 Sail parameters

Sail area	3 m^2
l_s center of pressure to sail hinge	5 m
E_s	0.05 (dimensionless)

Table 5 Design I dimension summary

$x_{a-cm} = y_{a-cm} = z_{a-cm}$	10 cm
$r_{\text{antenna}-x} = r_{\text{antenna}-z}$	0.725 m
$r_{\text{antenna}-y}$	0.5 m
$A_1 = A_6$ antenna surface area	2.05 m
$A_2 = A_3 = A_4 = A_5$ antenna surface area	1.45 m^2
Solar panel r	0.25 m
Solar panel h	1.0 m
Solar panel y	0.25 m
Solar panel z	0.10 m

Gaussian noise, and a sensor sampling rate of once each minute is used to determine the pointing error and its derivative. Tables 1-5 summarize the parameters used in the simulation study.

The simulation results lend credence to the previous assumptions that gyroscopic coupling torques and cross-axis coupling torques are negligible compared to the sail attitude control torques. Note that for the example just discussed, the harmonic content of the error and its derivative is in the neighborhood of 10 deg/h. This rate is much higher than the angular velocity of the solar panels about their shafts, roughly 15 deg/h, and hence there is some coupling between the angular momentum of the satellilte and the angular momentum of the antenna, but the attitude control law is able to compensate for it.

The results presented here are representative of over 100 different simulations of the attitude control equations for both designs I and II. Satellite transient response to pointing errors such as those just described were checked at eight equally spaced times of year (starting with the winter solstice) and at four different initial times of day (midnight, six a.m., noon, and six p.m.) Finally, most runs were made with the sails misaligned in cant and pitch, the satellite center of mass misaligned, gravity gradient disturbance torques present, antenna sunlight pressure disturbance torques present, and sensor measurements corrupted by additive Gaussian noise. In all cases, the design was capable of aligning itself properly in the face of this set of challenges to within attitude sensor noise limits.

Appendix A: Coordinate Frames and Coordinate Transformations

Five different coordinate frames are useful in discussing the attitude control dynamics of designs I and II. Each of the following four coordinate frames have their origin at the satellite center of mass.

$(X_E - Y_E - Z_E)$: Nominally Earth-pointing coordinate frame, with the X_E axis aimed at the center of mass of the Earth, the Y_E axis perpendicular to the X_E axis and the orbital plane, and the Z_E axis parallel to the axis of rotation of the Earth

$(X_a - Y_a - Z_a)$: The antenna-electronics principal axes frame, nominally coincident with $(X_E - Y_E - Z_E)$

$(X_S - Y_S - Z_S)$: Nominally sun-pointing coordinate frame, with the X_s axis aimed at the center of the sun, the Y_s axis perpendicular to X_s and parallel to the ecliptic, and the Z_s axis normal to the ecliptic

$(X_b - Y_b - Z_b)$: The body-fixed axes frame, parallel to the solar panel principal axes frame and nominally coincident with $(X_s - Y_s - Z_s)$

The fifth coordinate frame has its origin at the center of mass of the kth $(k = 1,2)$ solar panel.

$(X_{pk} - Y_{pk} - Z_{pk})$: The principal axes frame for solar cell panel k $(k = 1,2)$, nominally parallel to $(X_s - Y_s - Z_s)$

Direction cosines from one coordinate frame to another are differentiated by a combination of mnemonic subscripts and superscripts. For example, the direction cosines from $(X_a - Y_a - Z_a)$ to $(X_b - Y_b - Z_b)$ are denoted by D_b^a where the superscript a denotes antenna axes and the subscript b denotes body-fixed axes. Direction cosines from Earth-pointing coordinates to sun-pointing coordinates can be expressed in terms of sines and cosines of Euler angles (ψ, θ, ϕ) where ϕ is the daily orbital position of the satellite and changes at a rate of $2\pi/24$ rad/h, θ is the angle of the axis of rotation of the Earth with the ecliptic and is assumed to be 23.5 deg, and ψ is the annual orbital position of the satellite which changes at a rate of $2\pi/(365.25 \times 24)$ rad/h.

Appendix B: Inertia Tensors

In $(X_a - Y_a - Z_a)$ the antenna electronics inertia tensor is diagonal, with the only nonzero elements $I_{axx}, I_{ayy}, I_{azz}$. In body-fixed axes $(X_b - Y_b - Z_b)$ this becomes

$$I_{ab} = A_b^a I_{aa} A_a^b \tag{B1}$$

In solar panel principal axes $(X_{pk} - Y_{pk} - Z_{pk})$ the kth solar panel inertia tensor is diagonal, with elements $(I_{pxx}, I_{pyy}, I_{pzz})$ on the diagonal and zeroes elsewhere. In body-fixed axes $(X_b - Y_b - Z_b)$ for design I, either solar panel inertia tensor takes the form

$$I_p = I_{pm} + I_{pk} \qquad (k = 1,2) \tag{B2}$$

$$I_{pm} = m_p D^I_{\text{nom}} I_I (D^I_{\text{nom}})^{-1} \tag{B3}$$

where m_p is the solar cell panel mass and

$$I_I = \begin{bmatrix} h^2 & 0 & -rh \\ 0 & r^2 + h^2 & 0 \\ -rh & 0 & r^2 \end{bmatrix} \qquad D^I_{\text{nom}} = \begin{bmatrix} \cos\psi & -\sin\psi & 0 \\ \sin\psi & \cos\psi & 0 \\ 0 & 0 & 1 \end{bmatrix} \tag{B4}$$

In body-fixed axes for design II either solar panel inertia tensor takes the form

$$I_p = I_{pm} + I_{pk} \tag{B5}$$

$$I_{pm} = m_p D^{II}_{\text{nom}} I_{II} (D^{II}_{\text{nom}})^{-1} \tag{B6}$$

$$I_{II} = \begin{bmatrix} h & 0 & 0 \\ 0 & h^2 & 0 \\ 0 & 0 & 0 \end{bmatrix} \qquad D^{II}_{\text{nom}} = \begin{bmatrix} \cos\gamma & 0 & \sin\gamma \\ 0 & 1 & 0 \\ -\sin\gamma & 0 & \cos\gamma \end{bmatrix}$$

$$\sin\gamma = \sin\theta \sin\psi \tag{B7}$$

Finally, the satellite inertia tensor becomes in $(X_b - Y_b - Z_b)$

$$I_{sat} = I_{ab} + 2I_p \tag{B8}$$

The diagonal elements fluctuate about their mean values over a twenty-four hour interval, but the magnitude of the fluctuation is felt to be negligible to first order, as confirmed by the computer simulation studies.

Appendix C: Sail Torques

Sunlight pressure striking a surface generates a force with three physically distinct components, a reflected, absorbed, and reradiated component. Only the reflected component will be dealt with here:

$$F_{\text{reflected}} = A(1 - E_s)(2I/c)(n \cdot s)^2(-n) \tag{C1}$$

where A is the surface area, E the surface emissivity, I the sunlight pressure constant (1380 W/m^2), c is the speed of light in vacuum (3×10^8 m/s), s is the unit vector pointing at the center of the sun, and n is the unit normal outward from the surface. If we define a_k as the cant angle with respect to X_b axis of sail k $(k = 1,\ldots,6)$ and b_k as the pitch angle about longitudinal axis of sail k $(k = 1,\ldots,6)$, then

$$n_k = \begin{bmatrix} \cos a_k \cos b_k \\ \sin a_k \cos b_k \\ \sin b_k \end{bmatrix} \quad (k = 1,4) \qquad n_k = \begin{bmatrix} \cos a_k \cos b_k \\ -\sin a_k \cos b_k \\ \sin b_k \end{bmatrix} \quad (k = 3,6) \tag{C2}$$

$$n_2 = \begin{bmatrix} \cos a_2 \cos b_2 \\ \sin b_2 \\ \sin a_2 \sin b_2 \end{bmatrix} \qquad n_5 = \begin{bmatrix} \cos a_5 \cos b_5 \\ \sin b_5 \\ -\sin a_5 \cos b_5 \end{bmatrix} \tag{C3}$$

The vectors from the satellite center of mass to the center of pressure of each sail are

$$r_1 = \begin{bmatrix} -r\cos\psi - l_s \sin a_1 \\ r\sin\psi + l_s \cos a_1 + y \\ h \end{bmatrix} \qquad r_4 = \begin{bmatrix} r\cos\psi - l_s \sin a_4 \\ -r\sin\psi + l_s \cos a_4 + y \\ h \end{bmatrix} \tag{C4}$$

$$r_2 = \begin{bmatrix} -r\cos\psi - l_s \sin a_2 \\ r\sin\psi \\ h + z + l_s \cos a_2 \end{bmatrix} \qquad r_5 = \begin{bmatrix} r\cos\psi - l_s \sin a_5 \\ -r\sin\psi \\ -h - z - l_s \cos a_5 \end{bmatrix} \tag{C5}$$

$$r_3 = \begin{bmatrix} -r\cos\psi - l_s \sin a_3 \\ r\sin\psi - l_s \cos a_3 - y \\ h \end{bmatrix} \qquad r_6 = \begin{bmatrix} r\cos\psi - l_s \sin a_6 \\ r\sin\psi - l_s \cos a_6 \\ h \end{bmatrix} \tag{C6}$$

In body-fixed axes the torque generated by sail k $(k = 1,\ldots,6)$

is given by T_k where

$$T_k = r_k \times F_k = A(1-E_s)(2I/c)(n_k \cdot s)^2 (n_k \times r_k) \quad \text{(C7)}$$

$$N_{\text{body}} = \sum_{k=1}^{6} T_k = \text{total sail torque} \quad \text{(C8)}$$

where the dot-product of the sun-pointing unit vector with each sail normal is carried out assuming all vectors are expressed in body-fixed axes.

Appendix D: Antenna Sunlight Disturbance Torques

The sunlight disturbance torques are due to reflected sunlight pressure, to absorbed sunlight, and to reradiated sunlight.[11]

Reflected Sunlight Pressure Torques

In antenna principal axes, vectors from the satellite center of mass to the surface of the antenna are

$$r_1 = -r_6 = \begin{bmatrix} r_{ax} \\ 0 \\ 0 \end{bmatrix} \quad r_2 = -r_4 = \begin{bmatrix} 0 \\ -r_{ay} \\ 0 \end{bmatrix} \quad r_3 = -r_5 = \begin{bmatrix} 0 \\ 0 \\ -r_{az} \end{bmatrix} \quad \text{(D1)}$$

The reflected sunlight force on each antenna face is denoted by F^r_{ka} where

$$F^r_{ka} = A_k(1-E_{sk})(2I/c)(s \cdot n_k)^2(-n_k) \quad (k=1,\ldots,6) \quad \text{(D2)}$$

where A_k is the surface area of face k, E_{sk} is the emissivity of surface k, n_k is the unit normal in $(X_a - Y_a - Z_a)$ pointing outward from surface k, and s is the sun-pointing unit vector in antenna principal axes. Combining all this, the reflected sunlight torque due to each face in $(X_a - Y_a - Z_a)$ is

$$T^r_{ka} = r_k \times F^r_{ka} \quad \text{(D3)}$$

The total reflected sunlight torque due to the antenna in body-fixed axes is then given by

$$T^r_{\text{ant}} = A^q_b \sum_{k=1}^{6} T^r_{ka} \quad \text{(D4)}$$

Absorbed Sunlight Pressure Torques

Sunlight generates a force when it is absorbed upon striking a surface,

$$F_{\text{absorb}} = AB(I/c)(s \cdot n)(-s) \quad \text{(D5)}$$

where A is the surface area of the surface, B is surface absorptivity, I is the solar pressure constant, c is the speed of light in vacuum, and s is the unit vector pointing outward from the surface. The absorbed sunlight pressure force on each antenna face in antenna principal axes is then

$$F^q_{ka} = A_k B_k (I/c)(s \cdot n)(-s) \quad \text{(D6)}$$

and the total torque is the sum of the individual torques, where the individual torques are given by the cross-product of r_k with F^q_{ka}.

Reradiated Sunlight Pressure Torque

Reradiated sunlight generates a force when it strikes a surface given by

$$F_{\text{rerad}} = A(I_R/c)(-n) \quad \text{(D7)}$$

where A is the surface A, I_R is the intensity of reradiated sunlight, c is the speed of light in vacuum, and n is the unit normal vector outward from the surface. To find I_R the temperature on the surface must be found as a function of time, then the Stefan-Boltzmann formula must be used:

$$I_R = E_s T^4 \sigma \quad \text{(D8)}$$

where E_s is the surface emissivity, σ is the Stefan-Boltzmann constant, and T is the surface temperature.

When sunlight does not strike a surface, there is no reflected or absorbed force. Each of the reflected and absorbed sunlight pressure torques for a given surface are multiplied by a function which is one when the surface is in sunlight and zero when it is not. This shadowing factor was included in the graphs of the reflected and absorbed antenna sunlight torques.

Acknowledgments

This work was done at the Center for Space Research, Massachusetts Institute of Technology, Cambridge, Mass.

References

[1] Sohn, R., "Attitude Stabilization by Means of Solar Radiation Pressure," *ARS Journal*, Vol. 29, May 1959, p. 368.

[2] Modi, V.J. and Pande, K.C., "Solar Pressure Control of a Dual-Spin Satellite," *Journal of Spacecraft and Rockets*, Vol. 10, June 1973, pp. 355-361.

[3] Modi, V.J. and Kumar, K., "Attitude Control of Satellites Using the Solar Radiation Pressure," *Journal of Spacecraft and Rockets*, Vol. 9, Sept. 1972, p. 711.

[4] Pande, K.C., "Attitude Control of Spinning Spacecraft by Radiation Pressure," *Journal of Spacecraft and Rockets*, Vol. 13, Dec. 1976, pp. 765-766.

[5] Goddard Space Flight Center, "A Conceptual Study of a UHF-VHF Hybrid Satellite for a Delta Launch Vehicle," unpublished memo.

[6] MacLellan, D.C., MacDonald, H.A., Waldron, P., and Sherman, H., "Lincoln Experimental Satellites 5 and 6," AIAA 3rd Com. Sat. Conf., Los Angeles, Calif., April 1970.

[7] Trudeau, N., Sarles, F., and Howland, B., "Visible Light Sensors for Circular Near Equatorial Orbits," AIAA 3rd Com. Sat. Conf., Los Angeles, Calif., April 1970.

[8] Abel, J., "Attitude Control and Structural Response Interaction," JPL Report 32-1461, 1970.

[9] Likins, P.W. and Ohkami, Y., "Appendage Model Coordinate Truncation Criteria in Hybrid Coordinate Dynamic Analysis," *Journal of Spacecraft and Rockets*, Vol. 13, Oct. 1976, pp. 611-617.

[10] Meirovitch, L., "A New Model Method for the Response of Structures Rotating in Space," Paper 74-002, 25th IAF Congress, Amsterdam, Sept. 1974; *ACTA Astronautica*, Vol. 2, July 1975, pp. 563-576.

[11] "Spacecraft Radiation Torques," NASA SP-8027, 1969.

[12] Athans, M. and Falb, P., *Optimal Control*, McGraw-Hill, New York, 1966.

[13] Flugge-Lotz, I., *Discontinuous and Optimal Control*, McGraw-Hill, New York, 1968.

[14] Nidney, R., "Gravity Torque on a Satellite of Arbitrary Shape," *ARS Journal*, Vol. 30, Feb., 1960, p. 203.

[15] Naumann, R., "The Near Earth Meteoroid Environment," NASA TN D-3717, 1966.